

## Nuclidic Mass Formula on a Spherical Basis with an Improved Even-Odd Term

Hiroyuki KOURA,<sup>1,3,5</sup> Takahiro TACHIBANA,<sup>2,3,5</sup> Masahiro UNO<sup>4,3</sup> and  
Masami YAMADA<sup>3</sup>

<sup>1</sup>*Advanced Science Research Center, Japan Atomic Energy Research Institute  
(JAERI), Ibaraki 319-1195, Japan*

<sup>2</sup>*Senior High School of Waseda University, Tokyo 177-0044, Japan*

<sup>3</sup>*Advanced Research Institute for Science and Engineering, Waseda University,  
Tokyo 169-8555, Japan*

<sup>4</sup>*Ministry of Education, Culture, Sports, Science and Technology, Tokyo 100-8959,  
Japan*

<sup>5</sup>*The Institute of Physical and Chemical Research (RIKEN), Saitama 351-0198,  
Japan*

(Received July 2, 2004)

A nuclidic mass formula composed of a gross term, an even-odd term and a shell term is presented as a revised version of the mass formula constructed by the present authors and published in 2000. The gross term has almost the same functional form as in the previous formula, but the parameter values in it are somewhat different. The even-odd term is treated more carefully, and a considerable improvement is realized. The shell term is exactly the same as the previous one; it was obtained using spherical single-particle potentials and by treating the deformed nucleus as a superposition of spherical nuclei. The new mass formula is applicable to nuclei with  $Z \geq 2$  and  $N \geq 2$ . The root-mean-square deviation from experimental masses is 666.7 keV, which is less than that of the previous mass formula, 689.8 keV.

### §1. Introduction

Nuclear masses are important quantities to determine the ground state properties and reactions. Since the formulation of the Weizsäcker-Bethe nuclear mass formula,<sup>1,2)</sup> many mass predictions have been made. At the present time, the main purpose of the study of mass formulas is to predict reliable masses of unknown nuclides, especially neutron-rich nuclides and the superheavy nuclides. Some recent mass formulas have been applied to calculations of fission barriers and  $r$ -process nucleosyntheses.

One way to reproduce the known nuclear mass values is to use mass systematics. For example, the mass formulas presented by Comay et al. and Jänecke et al.<sup>3)</sup> are based on Garvey-Kelson-like systematics,<sup>4)</sup> which take into consideration particle-hole configurations and yield accurate predictions of known experimental masses, though it is rather difficult to apply these formulas to unknown nuclei far from known ones. In the last decade, some mass predictions designed for wide nuclidic regions have been presented. Among these, we specifically mention two sophisticated mass formulas that give not only nuclear masses but also nuclear shapes

and fission barriers. One is the finite-range droplet model (FRDM, 1995) formula, which is composed of a macroscopic droplet term and a microscopic shell term.<sup>5)</sup> The macroscopic term is calculated using the finite-range droplet model (FRDM), while the shell term is calculated using the folded-Yukawa single-particle potential. The other is the formula obtained with the Hartree-Fock plus the BCS-type pairing method with the MSk7 Skyrme force (HFBCS-1, 2001).<sup>6)</sup>

Our group has for years been investigating the nuclidic mass formula, which is composed of two parts: one representing the general trend of the masses as a function of the proton and neutron numbers ( $Z, N$ ), and the other representing the deviations from this general trend.<sup>7)–10)</sup> It is natural to think of the latter part as shell energies in a broad sense, because it is caused by the shell structure and, the deformation of the nucleus, if such exists.

In the early stage of our investigation, the method of constructing the mass formula, particularly the shell part, was rather phenomenological, and the mass formulas given in Refs. 7)–9) include many adjustable parameters. For example, the mass formula in Ref. 9), which is referred to as the TUYU formula hereafter, has about 300 parameters, of which 266 are in the shell part, and were determined by comparison with the experimental mass data. However, such an approach is of no use in the region of superheavy nuclei, where few empirical data are available.

There are many nuclides with spherical ground states, while there are also many nuclides having deformed ground states with various degrees of deformation. A direct way of treating a deformed nucleus is to assume a deformed single-particle potential and put nucleons in it.<sup>11)</sup> This method is natural, but it requires so much computer time that the search for the best form of the deformed potential is rather difficult. In addition, there still seems to be a problem of treating the continuum and unbound states, which affects the extraction of shell energies for loosely-bound states, for example, such states in nuclei near the neutron (proton)-drip line.<sup>12)</sup> We instead take another approach, based on the phenomenological treatment and expect to obtain some different findings for properties of nuclei.

During the last decade, we have been investigating a method for obtaining shell energies and presented a new method for calculating shell energies from spherical single-particle potentials.<sup>10),13)</sup> In Ref. 10), we show that any nuclear shell energy with  $Z, N \geq 2$  can be calculated without using deformed potentials; the key point of this new method is to treat the deformed nucleus as a particular superposition of spherical nuclei. The mass formula obtained in this manner<sup>10)</sup> with the shell energies is referred to as the KUTY00 formula hereafter. The standard deviation of the KUTY00 mass formula from experimental masses compiled in 1995<sup>14)</sup> is 680 keV. We applied this formula to superheavy nuclei and briefly considered some properties of superheavy nuclei, such as single-particle levels, shell energies, alpha-decay  $Q$ -values and spontaneous fission.<sup>12),15)</sup>

It is well known that there is an even-odd stagger among nuclidic masses. In the mass formula presented in Refs. 7) and 8), this stagger is incorporated in the shell part, except for a small correction term for odd-odd nuclei. By contrast, in the TUYU formula,<sup>9)</sup> an even-odd term is introduced separately from the shell term; thus, the even-odd stagger is not so marked in the shell term. In the KUTY00 formula,<sup>10)</sup>

the method of deriving the shell term is quite different from those of the previous formulas.<sup>7)–9)</sup> During the course of this derivation, there is a step to incorporate a BCS-type pairing; however, to reduce the complexity of the computation, this step is employed mainly for even  $Z$  and for even  $N$ ; nuclei with odd  $Z$  and/or odd  $N$  are treated by interpolation from those with even  $Z$  and/or even  $N$ . Therefore, a considerable part of the even-odd stagger is missing in the shell energies of KUTY00, and we introduce an additional even-odd term, as is done in the TUYU case.

In Ref. 10), we mainly focus on a method for obtaining shell energies; the treatment of the other parts, in particular the additional even-odd part, is insufficient. Some unreasonable results appear around the proton- and neutron-drip lines. In this paper, we treat the even-odd term more carefully. In our previous mass formulas,<sup>9),10)</sup> the functional form of the even-odd term is rather simple, and the parameters in it are adjusted so as to reproduce the total ground state masses. In this paper, we consider “experimental” even odd energies obtained from experimental masses and the gross and shell parts of the mass formula. We then construct a new even-odd term, aided by a comparison with these “experimental” even-odd energies. In this process, we find a significant property of the “experimental” even-odd energies. This is discussed in §3.2.

In §2 we present an explicit form of the gross term in the mass formula and only give an outline of the method for obtaining the shell energies, since this method is explained in detail in Ref. 10). In the present formula we use exactly the same shell term as in KUTY00. In §3, we explain how to obtain the “experimental” even-odd energies and construct the even-odd term. Section 4 is devoted to the determination of the parameter values for the even-odd term and the gross term. In §5, we elucidate some properties of the present mass formula. Concluding remarks are presented in §6.

## §2. Gross term and shell term

### 2.1. Gross term

Our mass formula consists of three parts,

$$M(Z, N) = M_g(Z, N) + M_{eo}(Z, N) + M_s(Z, N), \quad (2.1)$$

where  $M_g(Z, N)$  is the term representing the gross features of the nuclear mass surface,  $M_{eo}(Z, N)$  the even-odd term, and  $M_s(Z, N)$  the shell term.

The gross term expressed in energy units is taken as

$$\begin{aligned} M_g(Z, N)c^2 = & M_H c^2 Z + M_n c^2 N + a(A)A \\ & + b(A)|N - Z| + c(A)(N - Z)^2/A \\ & + E_C(Z, N) - k_{el}Z^{2.39}. \end{aligned} \quad (2.2)$$

Here,  $M_H$  and  $M_n$  are the mass excesses of a hydrogen atom,  ${}^1\text{H}$ , and a neutron, respectively, and  $A$  is the mass number,  $Z + N$ . This expression of the gross term is the same as Eq. (2) of Ref. 9), but here we have made small modifications to the

constants and coefficients. For  $a(A)$ ,  $b(A)$  and  $c(A)$ , we assume

$$\begin{aligned} a(A) &= a_1 + a_2 A^{-1/3} + a_3 A^{-2/3} + a_4 (A + \alpha_a)^{-1}, \\ b(A) &= b_1 + b_2 A^{-1/3} + b_3 A^{-2/3} + b_4 (A + \alpha_b)^{-1}, \\ c(A) &= c_1 + c_2 A^{-1/3} + c_3 A^{-2/3} + c_4 (A + \alpha_c)^{-1}. \end{aligned} \quad (2.3)$$

The parameters  $\alpha_a$ ,  $\alpha_b$ , and  $\alpha_c$  are introduced in order to avoid a drastic change of the gross term in the region of small mass numbers. The quantities  $a_j$ ,  $b_j$ ,  $c_j$ , ( $j = 1-4$ ),  $\alpha_a$ ,  $\alpha_b$ , and  $\alpha_c$  are parameters to be determined from experimental mass data, and their values are given in §4. The forms of the Coulomb term  $E_C(Z, N)$  and the binding energy of electrons with  $k_{\text{el}} = 14.33 \times 10^{-6}$  MeV in Eq. (2.2) are taken to be exactly the same as in Ref. 9).

## 2.2. Shell term

The shell term of our mass formula is the same as that in KUTY00, and it is obtained through the following procedure. First, spherical single-particle potentials are prepared for the neutrons and protons, and crude shell energies are deduced from the sums of the single-particle energies for the neutron groups and for the proton groups. Next, we modify these crude shell energies by taking into account the BCS-type pairing. Then, we apply a phenomenological reduction to these modified shell energies. The neutron and proton shell energies of this stage, which we refer to as refined spherical shell energies, are the final results for spherical nuclei. For deformed nuclei, we further mix these refined spherical shell energies in a suitable way to obtain the final shell energies. The details of this procedure are given in Ref. 10).

## §3. Even-odd term

First, we point out two causes for the even-odd effect in nuclear masses. One is that the nucleus has, at least partially, a certain kind of single-particle structure. The other is the existence of a strongly attractive nuclear central force in the singlet-even state (isospin-triplet spin-singlet state). This force is considered to be most effective among various types of nuclear forces for the nucleon pairing. A part of the effect of this force appears as the pairing in the  $j$ - $j$  coupling. The BCS-type pairing is also caused mainly by this force.

Here, we consider the single-particle structure of a nucleus in some detail. In the single-particle model, the degeneracy of each single-particle level is even. Because a nucleon is a fermion, the nucleons in the ground state of the nucleus fill the single-particle levels from the bottom. From this picture, we can understand that, in the extreme single-particle model, the ground state energy of a nucleus with an even number of protons (neutrons) is lower than that with an odd number of protons (neutrons), on the average. As a simple example, we consider a sequence of uniformly spaced single-particle energy levels with two-fold degeneracy. When  $n$  nucleons fill these levels from the lowest, which is taken to be zero, the sum of the single-particle

energies is given as

$$E_{\text{sp}}(n) = \begin{cases} n(n/2 - 1)d & \text{for even } n, \\ n(n/2 - 1)d + d/2 & \text{for odd } n, \end{cases} \quad (3.1)$$

with  $d$  being half of the energy-level spacing. This means that there exists an even-odd energy of  $d/2$  in this case.

We now turn to actual nuclei. In the region of deformed nuclei, the degeneracy of each single-particle level is two-fold, although the level distribution is not uniform. Therefore, we can expect a contribution to the even-odd term similar to that in the above simple example. Here and in the following,  $d$  should be taken as the spacing of the hypothetical non-degenerate, uniformly distributed single-particle levels around the Fermi surface. It depends strongly on the mass number, decreasing rapidly as  $A$  increases.

Many of the single-particle levels in spherical nuclei have a more than two-fold degeneracy. In such a case, the sum of the single-particle energies has a different feature, namely that no even-odd zigzag is apparent. This feature is appropriately called the shell effect. Yet, as seen from the fact that the magic numbers are all even, these sums are smaller, on the average, for nuclei with even  $Z$  ( $N$ ) than for those with odd  $Z$  ( $N$ ). Therefore, it can be said that some even-odd effect is hidden in the shell effect.

The above consideration suggests that the shell effect and the even-odd effect are not clearly separated. However, if the shell term is fixed in a certain way, the even-odd term can be determined.

### 3.1. "Experimental" values for the even-odd term

In this subsection we prepare data with which the even-odd term can be compared. For brevity, we define

$$M_{\text{gsh}}(Z, N) \equiv M_{\text{g}}(Z, N) + M_{\text{s}}(Z, N). \quad (3.2)$$

Then, Eq. (2.1) can be written

$$M(Z, N) = M_{\text{gsh}}(Z, N) + M_{\text{eo}}(Z, N). \quad (3.3)$$

In Eq. (3.2), the shell part,  $M_{\text{s}}(Z, N)$ , is already determined, actually taken from KUTY00. It has no apparent even-odd stagger, as mentioned above. The gross part,  $M_{\text{g}}(Z, N)$ , is not yet determined, but we can tentatively take an expression, e.g., from KUTY00. The problem concerning the choice of the gross part is discussed at the end of this subsection.

The even-odd part is expressed as

$$M_{\text{eo}}(Z, N) = M_{\text{odd}Z}(Z, N)\delta_{\text{odd}Z} + M_{\text{odd}N}(Z, N)\delta_{\text{odd}N} - M_{\text{oo}}(Z, N)\delta_{\text{odd}Z}\delta_{\text{odd}N}, \quad (3.4)$$

with

$$\delta_{\text{odd}Z} = \begin{cases} 0 & \text{for } Z\text{-even,} \\ 1 & \text{for } Z\text{-odd,} \end{cases} \quad (3.5)$$

$$\delta_{\text{odd}N} = \begin{cases} 0 & \text{for } N\text{-even,} \\ 1 & \text{for } N\text{-odd,} \end{cases} \quad (3.6)$$

where,  $M_{\text{odd}Z}(Z, N)$ ,  $M_{\text{odd}N}(Z, N)$ , and  $M_{\text{oo}}(Z, N)$  are assumed to be smooth functions of  $Z$  and  $N$ . In the following, we proceed by assuming that  $M_{\text{gsh}}(Z, N)$  is fixed.

We first consider the data used to determine  $M_{\text{odd}N}(Z, N)$ . When  $Z$  is even and  $N$  is odd, we can express the masses of the nuclei  $(Z, N - 1)$ ,  $(Z, N)$  and  $(Z, N + 1)$  as

$$M(Z, N - 1) = M_{\text{gsh}}(Z, N - 1), \quad (3.7)$$

$$M(Z, N) = M_{\text{gsh}}(Z, N) + M_{\text{odd}N}(Z, N), \quad (3.8)$$

$$M(Z, N + 1) = M_{\text{gsh}}(Z, N + 1). \quad (3.9)$$

In order to obtain “experimental” values of  $M_{\text{odd}N}(Z, N)$ , we use experimental masses, denoted by  $M^{\text{exp}}(Z, N)$ , etc., on the left-hand sides of Eqs. (3.7)–(3.9). Then, the “experimental” value of the odd- $N$  term is obtained as

$$\begin{aligned} M_{\text{odd}N}^{\text{exp}}(Z, N) &= M^{\text{exp}}(Z, N) - M_{\text{gsh}}(Z, N) \\ &\quad - \frac{1}{2}[M^{\text{exp}}(Z, N - 1) - M_{\text{gsh}}(Z, N - 1)] \\ &\quad - \frac{1}{2}[M^{\text{exp}}(Z, N + 1) - M_{\text{gsh}}(Z, N + 1)]. \end{aligned} \quad (3.10)$$

The reason we use Eq. (3.10) instead of

$$M_{\text{odd}N}^{\text{exp}}(Z, N) = M^{\text{exp}}(Z, N) - M_{\text{gsh}}(Z, N), \quad (3.11)$$

which is obtained from only Eq. (3.8), is as follows. The deviation of the current mass formulas from the experimental masses is several hundred keV in energy units, and the absolute value of  $M_{\text{odd}N}(Z, N)$  is of a similar magnitude. If we use Eq. (3.11), the “noise” will be comparable to the original “signal.” In Eq. (3.10), the “noise” is considerably reduced because, in general, the trends of the differences between the experimental masses and the mass formula are similar among neighboring nuclei. In Eq. (3.10), the “noise” is reduced by subtracting the average “noise” of  $M(Z, N - 1)$  and  $M(Z, N + 1)$ , and we can obtain a reasonable “experimental” value for the odd- $N$  term. For  $M_{\text{odd}Z}(Z, N)$ , we obtain “experimental” values by using a similar procedure.

Finally, we treat  $M_{\text{oo}}(Z, N)$  in Eq. (3.4). When both  $Z$  and  $N$  are odd, the “experimental” values of  $M_{\text{oo}}^{\text{exp}}(Z, N)$  are expressed with Eqs. (3.3) and (3.4) as

$$M_{\text{oo}}^{\text{exp}}(Z, N) = -M^{\text{exp}}(Z, N) + M_{\text{gsh}}(Z, N) + M_{\text{odd}Z}^{\text{exp}}(Z, N) + M_{\text{odd}N}^{\text{exp}}(Z, N). \quad (3.12)$$

Here, we assume that  $M_{\text{odd}N}^{\text{exp}}(Z, N)$  is linear for odd- $Z$  and odd- $N$ . This is expressed as

$$M_{\text{odd}N}^{\text{exp}}(Z, N) = \frac{1}{2}[M_{\text{odd}N}^{\text{exp}}(Z - 1, N) + M_{\text{odd}N}^{\text{exp}}(Z + 1, N)], \quad (3.13)$$

where the terms on the right-hand side of the equation can be replaced by Eq. (3.10), because all the pairs of values in the parentheses are even- $Z$  and odd- $N$ . The term  $M_{\text{odd}Z}^{\text{exp}}(Z, N)$  for odd- $Z$  and odd- $N$  can be expressed in a similar way. The values of  $M_{\text{oo}}^{\text{exp}}(Z, N)$  are obtained as

$$\begin{aligned}
 M_{\text{oo}}^{\text{exp}}(Z, N) = & \frac{1}{2}[M^{\text{exp}}(Z-1, N) + M^{\text{exp}}(Z, N-1) \\
 & + M^{\text{exp}}(Z, N+1) + M^{\text{exp}}(Z+1, N)] \\
 & - \frac{1}{4}[M^{\text{exp}}(Z-1, N-1) + M^{\text{exp}}(Z-1, N+1) \\
 & + M^{\text{exp}}(Z+1, N-1) + M^{\text{exp}}(Z+1, N+1)] \\
 & - M^{\text{exp}}(Z, N) \\
 & - \frac{1}{2}[M_{\text{gsh}}(Z-1, N) + M_{\text{gsh}}(Z, N-1) \\
 & + M_{\text{gsh}}(Z, N+1) + M_{\text{gsh}}(Z+1, N)] \\
 & + \frac{1}{4}[M_{\text{gsh}}(Z-1, N-1) + M_{\text{gsh}}(Z-1, N+1) \\
 & + M_{\text{gsh}}(Z+1, N-1) + M_{\text{gsh}}(Z+1, N+1)] \\
 & + M_{\text{gsh}}(Z, N).
 \end{aligned} \tag{3.14}$$

These “experimental” data are used as input data for constructing the even-odd term of our mass formula.

As stated above, we need a gross term in order to calculate the “experimental” even-odd energies and to determine the even-odd term. On the other hand, the gross term should be determined by a comparison with the mass data after the shell and even-odd terms are fixed. This problem is solved by employing an iteration method. We start with the gross term of KUTY00 and calculate the first approximation of the “experimental” even-odd energies, with which the first approximation of the even-odd term is obtained. Then, we calculate the first approximation of the gross term, with which the calculation of the second approximation starts. The values obtained with this procedure quickly converge; even the first approximations of the “experimental” even-odd energies and the even-odd term are very close to the final ones.

### 3.2. Comparison of the “experimental” even-odd energies between mirror nuclei

In the derivation of the gross term and the shell term, which are necessary to obtain the “experimental”  $M_{\text{odd}N}^{\text{exp}}(Z, N)$  [Eq. (3.10)] and  $M_{\text{odd}Z}^{\text{exp}}(Z, N)$ , we have carefully treated the charge symmetry. Then, it is interesting to compare the “experimental”  $M_{\text{odd}N}^{\text{exp}}(Z, N)$  and  $M_{\text{odd}Z}^{\text{exp}}(Z, N)$  between mirror nuclei. The charge symmetry of the nuclear force requires that these quantities are nearly equal.

There are 45 pairs of mirror nuclei in the experimental data table<sup>16)</sup> for which we can obtain “experimental”  $M_{\text{odd}N}^{\text{exp}}(Z, N)$  and  $M_{\text{odd}Z}^{\text{exp}}(Z, N)$ . The average of  $M_{\text{odd}N}^{\text{exp}}(a, b)c^2 - M_{\text{odd}Z}^{\text{exp}}(b, a)c^2$  (where  $a$  is even and  $b$  is odd) is about 100 keV, which is considerably smaller than the average of the even-odd term itself in this mass region (a few MeV). In Fig. 1,  $M_{\text{odd}N}^{\text{exp}}(a, b)c^2 - M_{\text{odd}Z}^{\text{exp}}(b, a)c^2$  are plotted. As

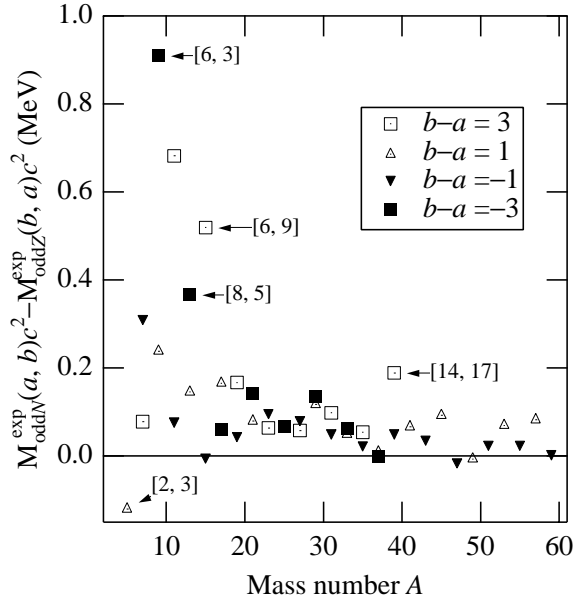


Fig. 1. Differences between the “experimental” even-odd energies for mirror nuclei,  $M_{\text{odd}N}^{\text{exp}}(a, b)c^2 - M_{\text{odd}Z}^{\text{exp}}(b, a)c^2$  ( $a$  is even, and  $b$  is odd. ( $a, b$ ) and ( $b, a$ ) represent ( $Z, N$ )). Some sets with larger and smaller values are indicated by  $[a, b]$ .

can be seen, almost all of these values are positive. This means that the even-odd term for a proton is somewhat smaller than that for a neutron. Undoubtedly, the main reason for this is the Coulomb repulsive force between protons; we believe the fact that  $M_{\text{odd}N}^{\text{exp}}(a, b)c^2 - M_{\text{odd}Z}^{\text{exp}}(b, a)c^2$  is positive is due to two mechanisms. One is related to the radius of the potential well. The radius of the single-proton potential, which is composed of the average nuclear potential and the average Coulomb potential, is larger than the single-neutron potential, and, accordingly, the single-particle level spacing, which serves as a measure of the even-odd energy, is narrower for a proton than for a neutron. The other mechanism is related to the proton-proton interaction in the pair. When two protons form a pair, the Coulomb repulsive force between them counteracts the attractive nuclear force. The above described feature of the “experimental” even-odd energies are taken into account when we construct the functional form of the even-odd term in the next subsection.

The Coulomb repulsive force has another effect: It expands the nucleus and makes the single-particle level spacing narrower for a proton as well as for a neutron. When this expansion is compared among isobars, a nucleus containing relatively many protons should undergo a larger expansion. Therefore, the effect of this expansion on the difference  $M_{\text{odd}N}^{\text{exp}}(a, b) - M_{\text{odd}Z}^{\text{exp}}(b, a)$  (with  $a + b = A$  fixed) should be to increase it for  $a < b$  and decrease it for  $a > b$ . We looked for such an effect in our data, but we could not find clear evidence of it.

We should mention another consideration of the BCS-type pairing effects for the above properties. The nuclei that we now examine are light nuclei, with  $A < 60$ , and these level densities are believed to be relatively small. Therefore it seems that



the BCS-type pairing effects are not large. The effect of the pairing energy from the two-fold degeneracy mentioned above is expected to be larger than that of the BCS-type pairing. This tendency is expected to reverse along the direction of increasing mass number  $A$ , because the level densities become larger in this direction. We can also see such an  $A$  dependence in Fig. 1.

### 3.3. Functional form of the even-odd term

In this subsection, we determine the functional form of  $M_{eo}(Z, N)$ . First, we consider the half-level spacing  $d$  near the Fermi surface. Suppose that neutrons occupy energy levels as in a degenerate Fermi gas in a volume  $V_n$ . When the neutron number  $N$  is sufficiently large, half of the amount by which the Fermi surface rises when the neutron number increases by 1 is calculated as

$$\frac{d_n}{2} \approx \frac{\pi^2 \hbar^2}{2m_n (3\pi^2 N)^{1/3} V_n^{2/3}}, \quad (3.15)$$

where  $m_n$  is the neutron mass. As mentioned above, this quantity is a certain measure of  $M_{\text{odd}N}(Z, N)$ . For the volume  $V_n$ , we take

$$V_n = \frac{4\pi}{3} R_n^3, \quad (3.16)$$

with

$$R_n = r_0 (A + A_{\text{ad}})^{1/3} \left( 1 + c_{\text{rq}} \left( \frac{N - Z}{A} \right)^2 \right) + r_{\text{ad}} + r_I \frac{N - Z}{A} + r_q \left( \frac{N - Z}{A} \right)^2, \quad (3.17)$$

where  $r_0$ ,  $A_{\text{ad}}$ ,  $c_{\text{rq}}$ ,  $r_{\text{ad}}$ ,  $r_I$ ,  $r_q$  are constants. The term with  $c_{\text{rq}}$  is introduced using the assumption that the equilibrium density of nuclear matter decreases as  $((N - Z)/A)^2$  increases. In our calculation, we take

$$c_{\text{rq}} = 1, \quad (3.18)$$

$$r_0 = 1.04 \text{ fm}. \quad (3.19)$$

The reason that we use a value of  $r_0$  which is slightly smaller than the typical value, 1.08 fm, is because we introduce the term with  $c_{\text{rq}}$ . In Eq. (3.17),  $A_{\text{ad}}$  is an adjustable parameter introduced to add freedom to the  $A$  dependence of the effective nuclear radius in the region of light nuclei. The remaining terms with  $r_{\text{ad}}$ ,  $r_I$ , and  $r_q$  are introduced to represent the effect of the structure of the nuclear surface. These parameters are treated as adjustable parameters, but not quite freely; we limit the ranges of the parameter values for  $r_I$  and  $r_q$  by requiring  $r_I \leq 3$  fm and  $r_q \leq r_I/2$  so that  $R_n$  does not change drastically with  $(N - Z)/A$ .

For the proton, we use  $d_p/2$ ,  $V_p$  and  $R_p$  given by expressions similar to (3.15)–(3.17) obtained by substituting the subscript p for n and by exchanging  $N$  and  $Z$  with the proton mass  $m_p$ . The parameter values of  $r_{\text{ad}}$ ,  $r_I$  and  $r_q$  for a proton might

be somewhat different from those for a neutron. However, we adopt the same values for the proton and neutron in order to limit the number of adjustable parameters.

With the above preparation we determine the functional form of the even-odd term. As mentioned above, the even-odd energies are approximately equal to  $d_p/2$  and  $d_n/2$  in the extreme single-particle model, although they may be hidden in the shell energies. Because we reduced the shell energies in the course of deriving the final shell term, the hidden even-odd energies have also been reduced. This is one of the reasons for introducing the even-odd term in our mass formula; if we consider the properties of the nuclear forces, it is clear that we need an even-odd term that compensates for the above-mentioned reduction of the (hidden) even-odd energy, because the strongly attractive nuclear force in singlet-even states surely lowers the energies of the proton pair and neutron pair in the state of the angular momentum and parity of the pair  $0^+$ . A natural form of the even-odd term to overcompensate for the reduction of the even-odd energy is  $c_{1n}d_n/2$  for neutrons and  $c_{1p}d_p/2$  for protons, where  $c_{1n}$  and  $c_{1p}$  are constants. These forms are strongly  $A$  dependent, and they may be caused mainly by coupling within single-particle orbitals with the same value of  $j^\pi$  (where  $j$  is the angular momentum quantum number, and  $\pi$  the parity). In addition to such strongly  $A$  dependent even-odd energies, we know that there are even-odd energies with a weaker  $A$  dependence. The latter are mainly caused by the BCS-type pairing, in which the single-particle orbitals with various  $j^\pi$  participate. It is not yet clear whether the BCS coupling in nuclei is a bulk effect or a surface effect. Therefore, we assume less strongly  $A$  dependent even-odd energies in the forms  $c_{2n}(d_n[\text{in MeV}]/2)^\alpha$  and  $c_{2p}(d_p[\text{in MeV}]/2)^\alpha$ , where  $c_{2n}$ ,  $c_{2p}$ , and  $\alpha$  are constants, and  $\alpha$  should be much less than unity. Thus, we have

$$M_{\text{odd}N}(Z, N)c^2 = c_{1n}d_n/2 + c_{2n}(d_n[\text{in MeV}]/2)^\alpha, \quad (3.20)$$

$$M_{\text{odd}Z}(Z, N)c^2 = c_{1p}d_p/2 + c_{2p}(d_p[\text{in MeV}]/2)^\alpha. \quad (3.21)$$

As mentioned in §3.2, the proton even-odd term is somewhat smaller than the neutron even-odd term. After some test calculations, we find that the coefficients in Eqs. (3.20) and (3.21) are related as

$$c_{1n} - c_{1p} = 0.05, \quad (3.22)$$

$$c_{2n} - c_{2p} = 0.02 \text{ MeV}. \quad (3.23)$$

After all, we represent  $M_{\text{odd}N}(Z, N)$  and  $M_{\text{odd}Z}(Z, N)$  by using seven adjustable parameters,  $A_{\text{ad}}$ ,  $r_{\text{ad}}$ ,  $r_I$ ,  $r_q$ ,  $c_{1n}$ ,  $c_{2n}$ , and  $\alpha$  with constraints on  $r_I$  and  $r_q$ .

Finally, we consider  $M_{\text{oo}}(Z, N)$ . This is caused by the interaction between the last odd-neutron and the last odd-proton. This interaction seems to be weaker than the pairing interaction, and  $M_{\text{oo}}(Z, N)$  should be smaller than either  $M_{\text{odd}Z}(Z, N)$  and  $M_{\text{odd}N}(Z, N)$ . We impose this constraint on the form of  $M_{\text{oo}}(Z, N)$ . For this purpose, we average  $M_{\text{odd}Z}(Z, N)$  and  $M_{\text{odd}N}(Z, N)$  with appropriate weights, and then multiply it by a function of  $Z$  and  $N$  with some upper limit. Actually, we take the reciprocal of each  $M_{\text{odd}Z}(Z, N)$  or  $M_{\text{odd}N}(Z, N)$  as the weight, and obtain

$$M_{\text{oo}}(Z, N) = f(Z, N) \frac{M_{\text{odd}Z}(Z, N) \cdot M_{\text{odd}N}(Z, N)}{M_{\text{odd}Z}(Z, N) + M_{\text{odd}N}(Z, N)}. \quad (3.24)$$

When we surveyed the “experimental” values of  $M_{oo}(Z, N)$ , almost all of them are positive, but those for  $Z = N$  are zero or negative. The reason for this exception may be the existence of the Wigner term in  $M_g(Z, N)$ . Because the Wigner term includes a factor  $|N - Z|$ , the nuclei with  $Z = N$  are more strongly bound than estimated by a smooth interpolation from neighboring nuclei, and some portion of the odd-odd effect may be included in the Wigner term. From this consideration, we assume that  $f(Z, N)$  in Eq. (3.24) includes  $(1 - \delta_{ZN})$  with  $\delta_{ZN}$  being the Kronecker delta. Then, we adopt the functional form for  $f(Z, N)$  as

$$f(Z, N) = (1 - \delta_{ZN})c_{oo}(1 + c_{oo1}(A^{-1/3} - A^{-2/3})), \quad (3.25)$$

where  $c_{oo}$  and  $c_{oo1}$  are adjustable parameters.

#### §4. Determination of adjustable parameters

##### 4.1. Parameters of the even-odd term

We determine the values of the adjustable parameters introduced in §3.3 by fitting the even-odd term to the “experimental” data obtained in §3.1. We mainly take the least-squares method. The values of nine adjustable parameters thus obtained are as follows:

$$\begin{aligned} A_{ad} &= 2, \quad r_{ad} = 0.1268 \text{ fm}, \\ r_I &= 3.0 \text{ fm}, \quad r_q = 1.4996 \text{ fm}, \\ c_{1n} &= 0.45, \quad c_{2n} = 1.6 \text{ MeV}, \quad \alpha = 0.25, \\ c_{oo} &= 0.1070, \quad c_{oo1} = 20.14. \end{aligned} \quad (4.1)$$

The root-mean-square (RMS) deviations of  $M_{oddZ}(Z, N)$  and  $M_{oddN}(Z, N)$  from the “experimental” values are 246.0 keV for 514 nuclei and 266.0 keV for 495 ones, respectively. The deviation of  $M_{oo}(Z, N)$ , excluding the case in which  $N = Z$ , is 153.3 keV for 402 nuclei.

Although we did not apply the same procedure to the even-odd term of the KUTY00 mass formula,<sup>10)</sup> we can calculate the “experimental” even-odd energies for KUTY00 by using its gross term. The RMS deviations of the even-odd term of KUTY00 from these “experimental” values are somewhat larger than the RMS deviation of the present even-odd term. The RMS deviation of  $M_{oddZ}(Z, N)$  is about 30% larger, and those of  $M_{oddN}(Z, N)$  and  $M_{oo}(Z, N)$  are about 20% larger.

Figure 2 displays the even-odd terms of KUTY00 and the present mass formula for Boron isotopes. The total even-odd term  $M_{eo}(Z, N)$  (plotted by solid curves in Fig. 2) exhibits zigzag behavior, in general, reflecting the fact that odd-odd nuclei are less strongly bound than in the case that they are interpolated from the neighboring odd- $Z$ -even- $N$  nuclei. In the upper figure for KUTY00, however, this zigzag behavior disappears, or it is even reversed for very neutron-rich nuclei,  $N = 15$  and (probably) 17, which are near or outside the neutron-drip line. This kind of behavior, which violates the rule of stability for even- $N$  (or even- $Z$ ) nuclei compared with odd- $N$  (or odd- $Z$ ) nuclei is unlikely to occur in actual nuclei, even though we do not have any

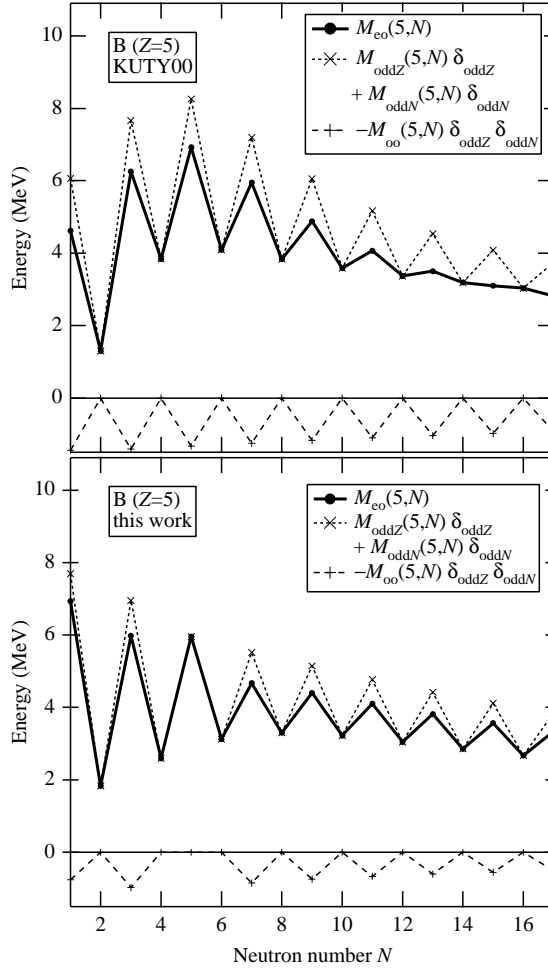


Fig. 2. Even-odd terms of B-isotopes in energy units for two mass formulas, KUTY00 and the present one. Because of the factor of  $1 - \delta_{ZN}$  in Eq. (3.25), the odd-odd term for  $Z = N$  is zero in the lower figure.

definite evidence to disprove it. On the other hand, the present even-odd term is designed so as to maintain the even-odd regularity, as seen in the lower figure. The situation is similar for  $Z, N = 3$  and  $5$ .

#### 4.2. Parameters of the gross term

In order to determine the values of the parameters in the gross term, we compare the calculated masses with the data set for the recommended mass values of Audi, Wapstra and Thibault in 2003,<sup>16)</sup> excluding those estimated by systematics. The nuclides with  $Z = 0, 1$  and/or  $N = 0, 1$  are excluded, because they are too light. Then, there are 2219 nuclides in all.

The parameters in the gross term are determined by the least-squares method in which we take the weight for each nuclide as  $1/(\Delta_i + 0.7 \text{ MeV})^2$ , where  $\Delta_i$  is the uncertainty in the experimental mass of this nuclide. If the absolute magnitude of

Table I. Parameters in the gross term in MeV obtained from a comparison with the data set Audi-Wapstra-Thibault03.<sup>16)</sup> The values in parentheses are the constrained ones.

$i$	1	2	3	4
$a_i$	-15.7528	15.9195	20.3540	(-40.00)
$b_i$	(0)	(0)	(0)	38.0024
$c_i$	27.6284	(-30.00)	(-30.0)	45.3567

a parameter becomes too large in this least-squares procedure, we constrain it to a reasonable magnitude so as not to cause a drastic variation in the region of light nuclei. Among the parameters in Eq. (2·3), we obtain  $\alpha_a = 1$ ,  $\alpha_b = 5$ ,  $\alpha_c = 10$ , and by considering the origin of the Wigner term, we set  $b_i = 0$  for  $i = 1-3$ . The improvement realized in this procedure mainly affects the light nuclei, and therefore there are some differences between these values and those for KUTY00. The values of the parameters thus determined are given in Table I.

In Fig. 3, we display the differences between the estimated masses obtained using the present and the KUTY00 mass formulas. This figure shows that nuclei with large differences are seen in the very neutron-rich region or in the region of very light nuclei. Differences on the  $N = Z$  line are also notable.

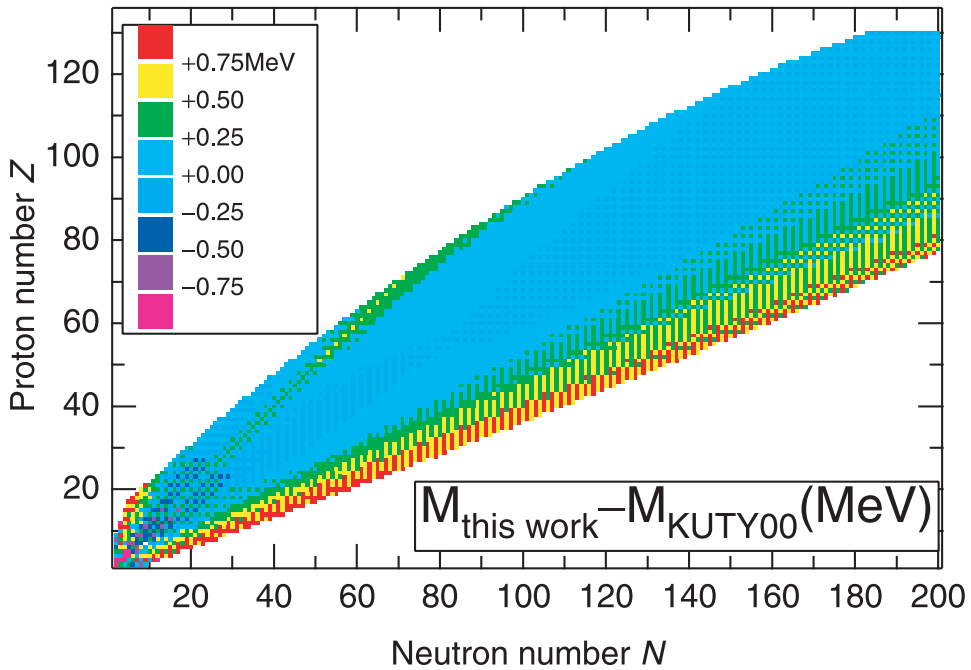


Fig. 3. Differences between the masses (in energy units) calculated using the present formula and KUTY00.<sup>10)</sup>

## §5. Properties of the mass formula

### 5.1. Masses, neutron and proton separation energies

The differences between the calculated masses and the experimental masses<sup>16)</sup> are shown in Fig. 4, and the RMS deviations are listed in Table II. The RMS deviation for our present formula is 666.7 keV for 2219 experimental masses, which is smaller than that of the KUYT00 mass formula,<sup>10)</sup> 689.8 keV. In Table II, we also list the RMS deviations for two other recently proposed mass formulas that make predictions of masses and deformations for nuclei in a wide nuclidic region, namely those of the finite range droplet model (FRDM),<sup>5)</sup> and the Hartree-Fock plus BCS pairing (HFBCS-1) model.<sup>6)</sup> Among these, our mass formula has the smallest RMS deviation. Although there is not much difference in the RMS deviations among these three mass formulas, there still remain fairly large differences among the estimated masses for some individual nuclides. The RMS deviations of the separation energies

Table II. RMS deviations of mass formulas from experimental data<sup>16)</sup> in keV.

Mass formula	nuclidic region	
	$Z, N \geq 2$ (2219 nuclei)	$Z, N \geq 8$ (2149 nuclei)
this work	666.7	652.8
KUTY00 <sup>10)</sup>	689.8	670.7
FRDM <sup>5)</sup>	-	655.5
HFBCS-1 <sup>6)</sup>	-	770.7

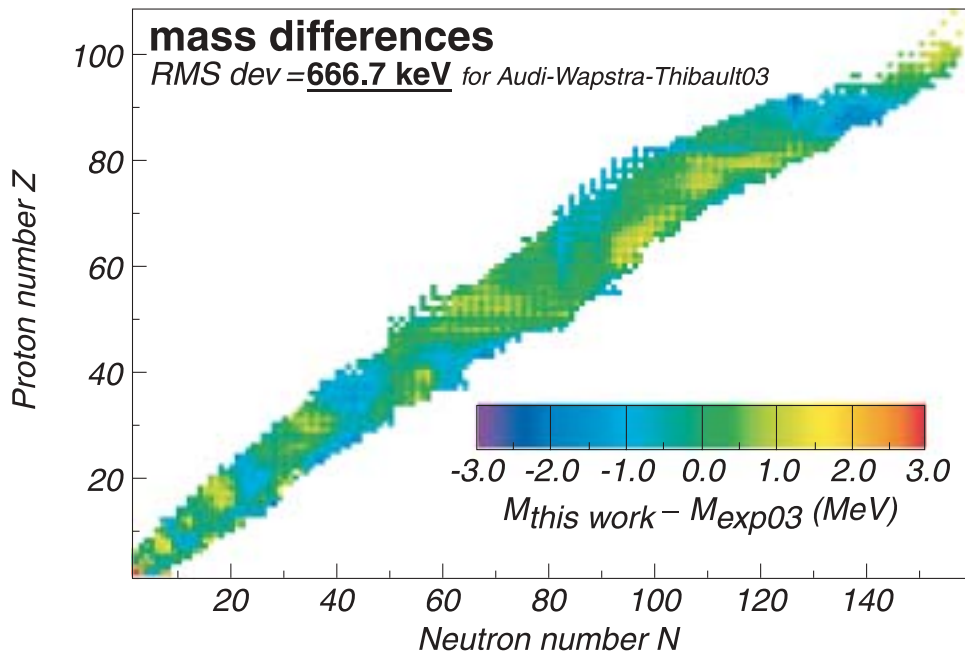


Fig. 4. Differences between the calculated masses and the experimental masses in energy units.

Table III. RMS deviations of the separation energies from experimental data<sup>16)</sup> for these mass formulas in keV. The values in parentheses are the numbers of nuclei.

Mass formula	neutron		proton	
	$S_n$	$S_{2n}$	$S_p$	$S_{2p}$
$Z, N \geq 2$	(2054)	(1997)	(2016)	(1897)
this work	352.9	442.0	389.9	532.2
KUTY00 <sup>10)</sup>	389.1	462.4	437.6	558.2
$Z, N \geq 8$	(1988)	(1937)	(1948)	(1835)
this work	316.2	379.1	353.0	490.1
KUTY00 <sup>10)</sup>	339.0	386.5	379.2	499.7
FRDM <sup>5)</sup>	399.3	511.7	395.2	493.6
HFBCS-1 <sup>6)</sup>	451.8	477.3	496.5	603.8

for our mass formula, including the previous formula, KUTY00, are listed in Table III together with those for the other two. It is seen that our RMS deviation is significantly smaller than those for the others.

The limit of the region of “stable” nuclei with respect to neutron or proton emission can be predicted with the separation energies as

$$\begin{aligned}
 &S_n > 0 \text{ and } S_{2n} > 0 \text{ on the neutron-rich side,} \\
 &S_p > 0 \text{ and } S_{2p} > 0 \text{ on the neutron-poor side.}
 \end{aligned}
 \tag{5.1}$$

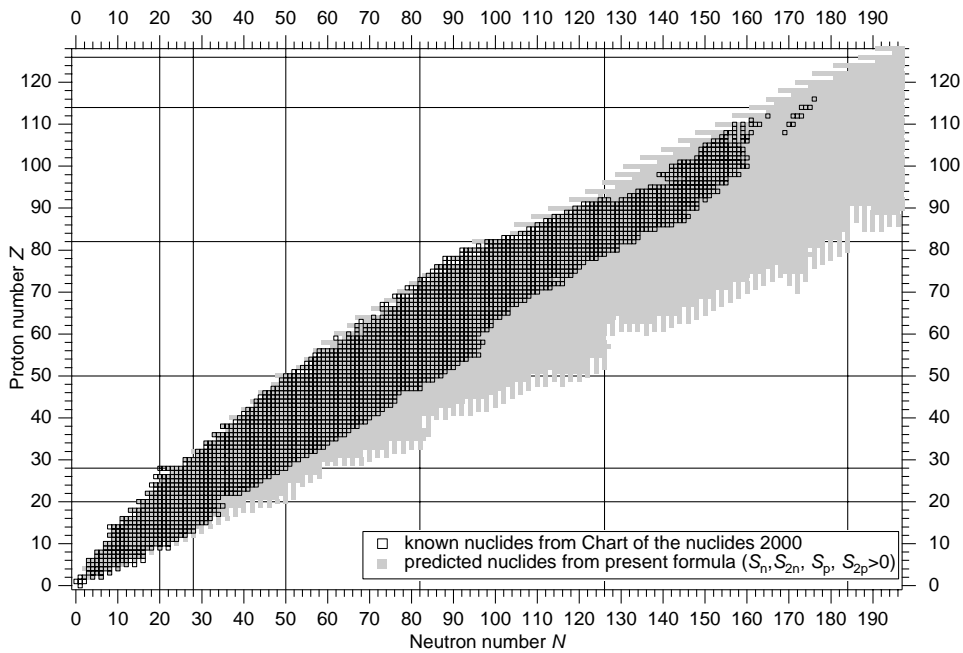


Fig. 5. Nuclei with  $S_n, S_{2n}, S_p, S_{2p} > 0$  predicted by the present mass formulas. The known nuclei from Ref. 18), which include the proton-emitting nuclei in the neutron-poor side, are also plotted as small boxes.

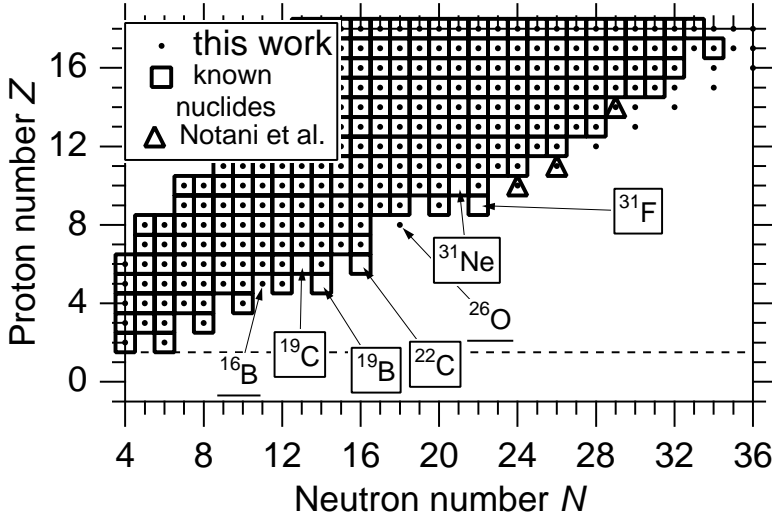


Fig. 6. Nuclei with  $S_n, S_{2n}, S_p, S_{2p} > 0$  predicted by the present mass formula in the region of light nuclei (dots). The known nuclei taken from Ref. 18) are also shown (squares). The seven nuclei exhibiting possible discrepancies between experiments and calculations are indicated by nuclidic symbols; the boxed symbols indicate the nuclei which have been confirmed experimentally to be stable with respect to particle emission, and the underlined symbols indicate nuclei unstable with respect to particle emission or unknown nuclei. The nuclei recently identified by Notani et al.,<sup>20)</sup>  $^{34}\text{Ne}$ ,  $^{37}\text{Na}$ ,  $^{43}\text{Si}$ , are also shown (triangles).

Table IV. Neutron separation energies obtained with the present mass formula for light nuclei near the neutron-drip line in MeV. Only nuclides with discrepancies between experiment and prediction are shown. The underlined values are of greatest interest.

nuclide	exp.	this work	
		$S_n$	$S_{2n}$
$^{16}\text{B}$	unknown <sup>18)</sup>	<u>+0.02</u>	+2.46
$^{26}\text{O}$	unstable <sup>19)</sup>	+1.40	<u>+0.21</u>
$^{19}\text{B}$	identified <sup>18)</sup>	+0.12	<u>-0.51</u>
$^{19}\text{C}$	identified <sup>18)</sup>	<u>-0.04</u>	+3.76
$^{22}\text{C}$	identified <sup>18)</sup>	+0.94	<u>-0.31</u>
$^{31}\text{F}$	identified <sup>18)</sup>	+0.45	<u>-0.47</u>
$^{31}\text{Ne}$	identified <sup>18)</sup>	<u>-0.58</u>	+2.35

Figure 5 displays results for nuclei with  $S_n, S_{2n}, S_p, S_{2p} > 0$ .

We also compare our neutron-drip line in detail with the experimental one in the region of light nuclei. Figure 6 displays the nuclides that are predicted to be stable with respect to particle emission and experimentally known nuclides.<sup>18)</sup> In the region satisfying  $10 \leq A \leq 31$ , the location of the estimated neutron-drip line is almost the same as that found experimentally. The discrepancies are as follows. Although our mass formula predicts that  $^{16}\text{B}$  and  $^{26}\text{O}$  are stable with respect to emission of one or two neutron, these nuclides are experimentally unknown or unstable. Contrastingly,  $^{19}\text{B}$ ,  $^{19}\text{C}$ ,  $^{22}\text{C}$ ,  $^{31}\text{F}$  and  $^{31}\text{Ne}$  are unstable according to our mass formula, but they have been experimentally identified. As listed in Table IV, the calculated values of



$|S_n|$  and  $|S_{2n}|$  for these nuclei are not very large. The underlined values in Table IV are within, or almost within, the RMS deviations of  $S_n$  and  $S_{2n}$  given in Table III; only the values of  $S_{2n}$  for  $^{19}\text{B}$  and  $S_n$  for  $^{31}\text{Ne}$  are 1.15 and 1.65 times as large as the RMS deviation of  $S_{2n}$  and  $S_n$ , respectively.

Recently, the neutron-rich isotopes  $^{34}\text{Ne}$ ,  $^{37}\text{Na}$  and  $^{43}\text{Si}$  were identified, and evidence for the particle instability of  $^{33}\text{Ne}$ ,  $^{36}\text{Na}$  and  $^{39}\text{Mg}$  was obtained.<sup>20)</sup> These experimental results are in agreement with predictions of the present mass formula.

### 5.2. Systematics of the separation energies

Figure 7 displays the two-neutron separation energies  $S_{2n}$ , the experimental data in the upper panel and our results in the lower panel. We connect the nuclei with the same  $N$  by solid lines. In such a figure, magicities are seen as large gaps between two lines. In the upper panel, we see large gaps between  $N = 8$  and 10 (abbreviated

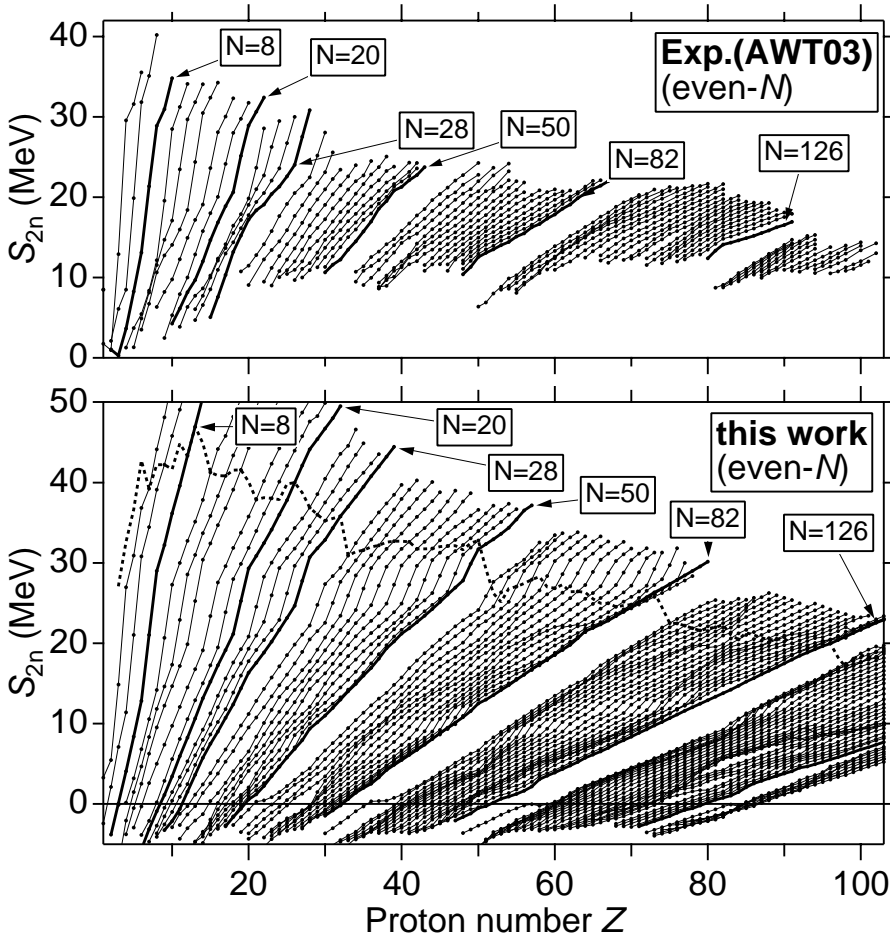


Fig. 7. Two-neutron separation energy  $S_{2n}$  for even  $N$ . The experimental values of  $S_{2n}$  are plotted in the upper figure, and the values of  $S_{2n}$  from the present mass formula are plotted in the lower figure. The solid lines connect nuclei with the same  $N$ , and the dashed line connects the lightest nuclei stable with respect to proton emission for fixed  $N$ .

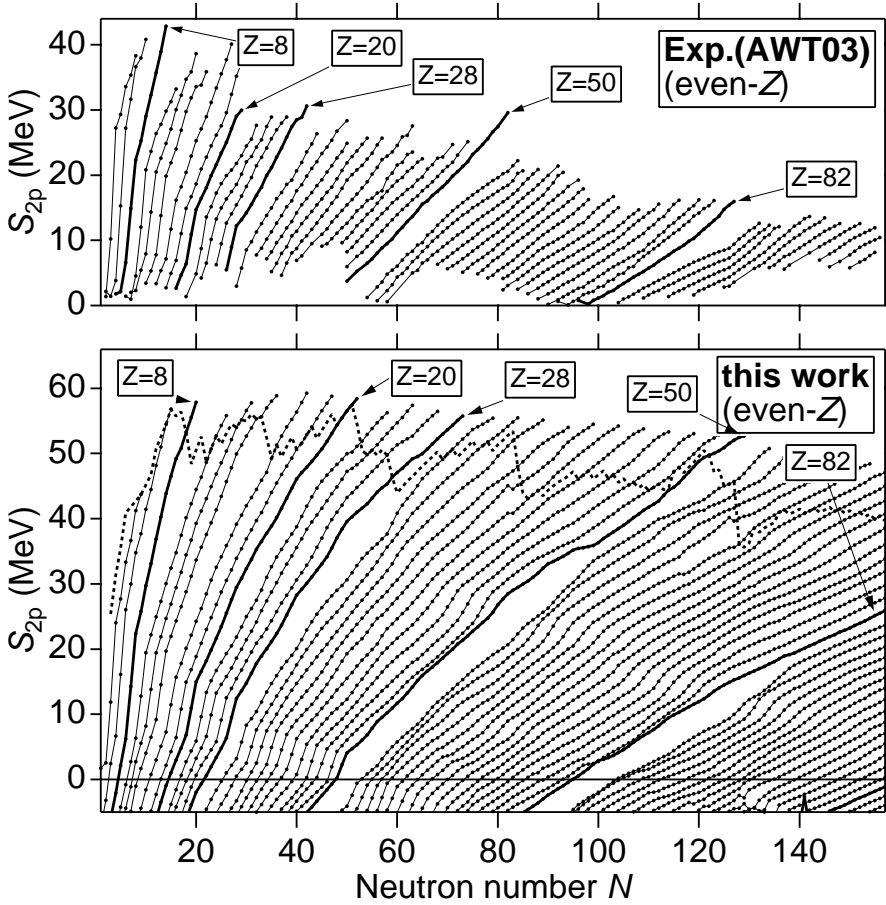


Fig. 8. Two-proton separation energy  $S_{2p}$  for even  $Z$ . The experimental values of  $S_{2p}$  are plotted in the upper figure, and the values of  $S_{2p}$  from the present mass formula are plotted in the lower figure. The solid lines connect the nuclei with the same  $Z$ , and the dashed line connects the lightest nuclei stable with respect to neutron emission for fixed  $Z$ .

“at  $N = 8$ ”), and at  $N = 20, 28, 50, 82, 126$ , except for the region with very small values of  $S_{2n}$ . Similar gaps are seen in the lower panel. In the very neutron-rich region, which corresponds to the region near the  $S_{2n} = 0$  line, the gaps of our  $S_{2n}$  at  $N = 20, 28, 50$  exhibit substantial decreases, while the gaps at  $N = 16, 32$  (or  $34$ ),  $58$  become larger compared with the neighboring ones.

Figure 8, like Fig. 7, displays the two-proton separation energies  $S_{2p}$ . Here, we connect the nuclei with the same  $Z$  by solid lines. In the upper panel of Fig. 8, large gaps are seen at the magic numbers  $Z = 8, 20, 28, 50, 82$ . Similar gaps are also seen in the lower panel. As we move to the very neutron-rich region, which corresponds to the region near the dashed line, the gap of our  $S_{2p}$  at  $Z = 82$  decreases, and the gap at  $Z = 50$  first decreases and then increases. By contrast, the gaps at  $Z = 8, 14$ , and  $20$  become larger than the neighboring ones. These properties are similar to those of KUTY00.

5.3. Nuclear deformation

We show our deformation parameter  $\alpha_2$  in Fig. 9. The present deformation parameters are the same as those of KUTY00, because, as mentioned above, the same shell energies are used for these two mass formulas. The deformation parameters  $\alpha_i$  can be converted into other deformation parameters  $\beta_i$  using the relation

$$\beta_i = \sqrt{4\pi/(2i + 1)}\alpha_i, \quad i = 2, 4, 6. \tag{5.2}$$

Compared with the experimental information regarding  $|\beta_2|$  derived from experimental  $B(E2)$ ,<sup>21)</sup> the calculated deformation is qualitatively in agreement with experiment in the sense that strongly deformed nuclei appear approximately in the right places in the  $N$ - $Z$  plane. Here, it should be noted that no nuclides are found to be exactly spherical; many nuclides, including the double-magic nuclides  $^{132}\text{Sn}$  and  $^{208}\text{Pb}$ , are found to be slightly prolate. This is due to the energy-favoring prolate shapes, Eq. (79) in Ref. 10). In practice, this deviation from spheres does not seem to pose a serious problem, because the calculated deformations in the nuclidic region when the nuclei are allowed to be spherical, are generally very small ( $\alpha_2 A \lesssim 1$ ).

When we look into the deformation more quantitatively, we find that the calculated deformations are not large enough. The RMS deviation of our  $|\beta_2|$  from the value of  $|\beta_{2\text{exp}}|$  derived from  $B(E2)$  is 0.137 for 324 even-even nuclei. This value is somewhat larger than those of FRDM and HFBCS-1, 0.106 and 0.126, respectively. We can also consider another indicator for the deviation, defined by

$$r_{\text{def}} \equiv \sqrt{\sum \beta_{2\text{th}}^2 / \sum |\beta_{2\text{exp}}|^2}, \tag{5.3}$$

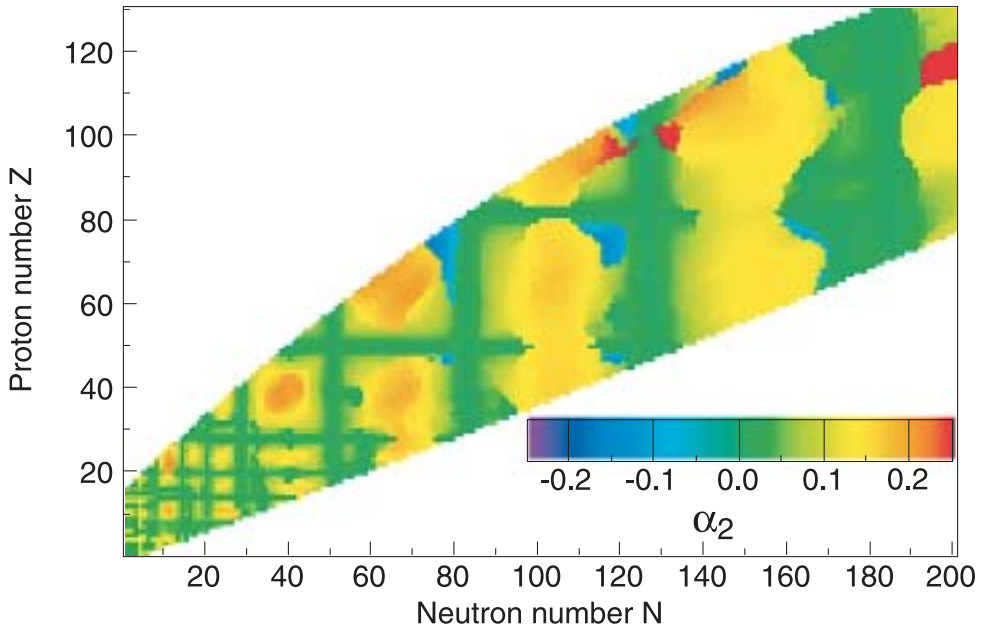


Fig. 9. Deformation parameter  $\alpha_2$ .

where the sums are taken over the nuclides for which both the theoretical and experimental values are available. When our values of  $\beta_2$  are used for  $\beta_{2\text{th}}$ , the indicator  $r_{\text{def}}$  is calculated to be 0.626. The smallness of this value compared to 1 is not so surprising, because nuclear vibration makes a partial contribution to  $B(E2)$ , and consequently to  $|\beta_{2\text{exp}}|^2$ , whereas it makes no contribution to our  $\beta_2$ . However, the above value is also smaller than those of FRDM and HFBCS-1 (0.757 and 0.789, respectively), which do not include a contribution from nuclear vibration either.

Improvement of the deformation is a future problem to be considered together with improvements in the mass values.

## §6. Concluding remarks

In the previous sections, we presented the revised version of our mass formula on a spherical basis published in 2000. In the new mass formula, the even-odd term is mainly revised. With this revision, this formula accurately predicts experimental results of the neutron-drip light nuclei within the predictability of this mass formula itself. In the process we pointed out a difference between the “experimental” even-odd term and between the neutron-neutron and proton-proton pairs. On the deviation from experimental masses, we found that our formula accurately predicts not only the experimental masses but also the first derivative of the masses as neutron and proton separation energies. Furthermore, we remark that the present formula results in supporting some changes of magicities toward the nuclidic region far from the  $\beta$ -stability line.

We have compiled a table which lists ground state masses, deformation parameters  $\alpha_2$ ,  $\alpha_4$ ,  $\alpha_6$ , shell energies, one- and two-neutron separation energies, and one- and two-proton separation energies for 9437 nuclei ranging from  $Z \geq 2$  and  $N \geq 2$  to  $Z \leq 130$  and  $N \leq 200$ . This table is available on the World-Wide Web at [http://wwwndc.tokai.jaeri.go.jp/nucldata/mass/KTUY05\\_m246S12np.pdf](http://wwwndc.tokai.jaeri.go.jp/nucldata/mass/KTUY05_m246S12np.pdf) and [http://wwwndc.tokai.jaeri.go.jp/nucldata/mass/KTUY05\\_m246.dat](http://wwwndc.tokai.jaeri.go.jp/nucldata/mass/KTUY05_m246.dat). The table will also be sent upon request.

## Acknowledgements

The numerical calculations were mainly done on the computer VX at the Media Network Center (MNC), Waseda University, and with the VPP700 at the Computer and Information Division, RIKEN. This work was financially supported by MNC of Waseda University as Specific Studies A in 2001, and it was partly supported by a Waseda University Grant for Special Research Projects (2003A-118).

## References

- 1) C. F. von Weizsäcker, *Z. Phys.* **96** (1935), 431.
- 2) H. A. Bethe and R. F. Bacher, *Rev. Mod. Phys.* **8** (1936), 829.
- 3) P. E. Haustein, *At. Data Nucl. Data Tables* **39** (1988), 185.
- 4) G. T. Garvey et al., *Rev. Mod. Phys.* **41** (1969), S1.
- 5) P. Möller, J. R. Nix, W. D. Myers and W. J. Swiatecki, *At. Data Nucl. Data Tables* **59** (1995), 185.

- 6) S. Goriely, F. Tondeur and J. M. Pearson, *At. Data Nucl. Data Tables* **77** (2001), 311.
- 7) M. Uno and M. Yamada, *Prog. Theor. Phys.* **65** (1981), 1322.
- 8) M. Uno, M. Yamada, Y. Ando and T. Tachibana, *Bulletin of Science and Engineering Research Laboratory, Waseda University No. 97* (1981), 19.
- 9) T. Tachibana, M. Uno, M. Yamada and S. Yamada, *At. Data Nucl. Data Tables* **39** (1988), 251.
- 10) H. Koura, M. Uno, T. Tachibana and M. Yamada, *Nucl. Phys A* **674** (2000), 47.
- 11) V. M. Strutinsky, *Nucl. Phys. A* **122** (1968), 1.
- 12) H. Koura, *Tours Symposium on Nuclear Physics V (TOURS2003)*, ed. M. Arnould et al., *AIP Conf. Proc.* **704** (AIP, New York, 2004), p. 60.
- 13) H. Koura and M. Yamada, *Nucl. Phys. A* **671** (2000), 96.
- 14) G. Audi and A. H. Wapstra, *Nucl. Phys. A* **595** (1995), 409.
- 15) H. Koura, *Tours Symposium on Nuclear Physics IV (TOURS2000)*, ed. M. Arnould et al., *AIP Conf. Proc.* **561** (AIP, New York, 2001), p. 388.
- 16) G. Audi, A. H. Wapstra and C. Thibault, *Nucl. Phys. A* **729** (2003), 337.
- 17) S. Raman, C. H. Malarkey, W. T. Milner, C. W. Nestor, Jr. and P. H. Stelson, *At. Data Nucl. Data Tables* **36** (1987), 1.
- 18) T. Horiguchi, T. Tachibana, H. Koura and J. Katakura, *Chart of the nuclides 2000*, Japan Atomic Energy Research Institute (2001).
- 19) A. Ozawa et al., *Nucl. Phys. A* **673** (2000), 411.
- 20) M. Notani et al., *Phys. Lett. B* **542** (2002), 49.
- 21) S. Raman, C. W. Nestor, Jr. and P. Tikkanen, *At. Data Nucl. Data Tables* **78** (2001), 1.